https://doi.org/10.1016/j.chemphys.2024.112220

How Much Does Thermal Nonequilibrium Influence the Overall Atomic Recombination During De-Excitation?

Sangdi Gu[1,a], Jiaao Hao[1], Chih-Yung Wen[1], Qizhen Hong[2] and Qiu Wang[2]

[1]Department of Aeronautical and Aviation Engineering, The Hong Kong Polytechnic University, Kowloon, Hong Kong, China.
[2]State Key Laboratory of High Temperature Gas Dynamics, Institute of Mechanics, Chinese Academy of Sciences, No. 15 Beisihuanxi Road, Beijing, 100190, China.

Abstract

A parametric study is carried out via state-to-state constant-volume heat bath simulations for binary mixtures of O_2/O and N_2/N to identify nonequilibrium de-excitation conditions where the overall atomic recombination is influenced by thermal nonequilibrium and where it is not. The most important parameter is found to be the translational temperature at which the de-excitation occurs. A low translational temperature of around 500 K is found to prevent the overall atomic recombination process from being influenced by the thermal nonequilibrium, due to the small value of K_{EQ} making the dissociation reaction less important. At a higher translational temperature of 2000 K, the overall atomic recombination process is influenced by the thermal nonequilibrium to an extent that is comparable to that seen in the corresponding excitation conditions, due to the nonequilibrium-accelerated dissociation rate. The current results have important implications in reduced-order modelling and experimental methods.

I. Introduction

High-enthalpy flows involve shock waves and expansions which rapidly change the flow's translational (kinetic) temperature by thousands of Kelvins. However, the internal energy and chemical modes require longer adjusting, resulting in a region of thermochemical nonequilibrium [1]. In the past decades, while nonequilibrium under excitation (post-shock) conditions has been well-studied, the reverse scenario of nonequilibrium under de-excitation (expansion) conditions has not been given the appropriate attention [2]. De-excitation nonequilibrium is important in the flow over the shoulder and afterbody of an atmospheric entry vehicle [3, 4], in hypersonic wind tunnels [5, 6], and in the boundary layer [7].

In reduced-order models, such as multi-temperature models [8], the finite-rate chemistry consisting of both the forward and backward reactions is usually modelled using global rate constants. The influence of thermal nonequilibrium on the global dissociation/recombination rate constants, for the dissociation/recombination

[a]Corresponding author. Email: sangdi.gu@polyu.edu.hk

reaction $AB + M \leftrightarrow A + B + M$, is a question that has been mentioned since at least the 1960s [9]. It is now known that the global recombination rate constant, K_R, is a function of only the translational temperature, T_{tr}, such that [10-12]

$$K_R = \frac{\sum_i k_d(i, T_{tr}) f_{eq}^{AB}(i, T_{tr})}{K_{EQ}(T_{tr})} \tag{1}$$

where k_d is the vibrational state-specific dissociation reaction rate constant (which is a function of the vibrational energy level i and the translational temperature), f_{eq}^{AB} is the normalized Boltzmann distributed (equilibrium) vibrational population distribution (normalized such that $\sum_i f_{eq}^{AB}(i) = 1$) of molecule AB at the translational temperature, and K_{EQ} is the equilibrium constant evaluated at the translational temperature. On the other hand, the global dissociation rate constant, K_D, is a function of both the translational temperature, T_{tr}, and the vibrational population distribution such that [10, 11]

$$K_D = \sum_i k_d(i, T_{tr}) f^{AB}(i) \tag{2}$$

where f^{AB} is the normalized vibrational population distribution of molecule AB. A nonequilibrium factor Z, which measures the deviation of K_D from the global dissociation rate constant at equilibrium K_D^{EQ}, is defined as

$$Z = \frac{K_D}{K_D^{EQ}} = \frac{\sum_i k_d(i, T_{tr}) f^{AB}(i)}{\sum_i k_d(i, T_{tr}) f_{eq}^{AB}(i, T_{tr})} \tag{3}$$

Inspection of the above equation shows that it can only equal 1 when the actual vibrational population of AB is Boltzmann distributed at the local translational temperature (thermal equilibrium) or when k_d is a constant for all values of i. The latter condition is never really achievable in reality, but it does indicate that the distribution of the value of the state-specific rate constant k_d plays an important role in determining the magnitude of the deviation of K_D from K_D^{EQ}. For the dissociation/recombination reactions, the state-specific rate constant at a given temperature increases with increasing vibrational energy level and the steepness of this increase decreases with increasing temperature as shown in Figure 1 for example.

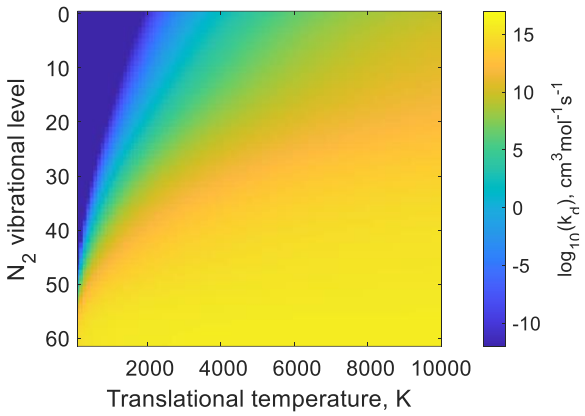

Figure 1. The state-specific rate constants for $N_2(i) + N \rightarrow 3N$ obtained via QCT [13].

The values of K_D^{EQ} are readily available in the literature [11]. One can then easily obtain the recombination rate constant via $K_R = K_R^{EQ} = \frac{K_D^{EQ}}{K_{EQ}(T_{tr})}$ with the equilibrium constant calculated using the partition functions; this approach has recently been further validated via detailed kinetics simulations [14]. The difficulty, therefore, lies in the determination of K_D. Because the dissociation reaction is dominant under excitation conditions, the accurate prediction of K_D is obviously important for simulating excitation conditions. As a result, various simple analytical models, being functions of only the translational and vibrational temperatures, have been developed and tuned to predict Z under relevant excitation conditions [11, 15, 16]. Under de-excitation conditions, these simple models do not work due to the strong non-Boltzmann distributions present [17, 18], so a much more sophisticated model is generally required to predict Z (and consequently K_D) correctly [7, 10, 19]. Nevertheless, it is not immediately obvious whether accurate dissociation reaction predictions are actually necessary under de-excitation conditions. On one hand, one may suggest that it is not important because the recombination reaction may be very dominant [12], in which case the prediction of the chemical nonequilibrium process becomes rather trivial as it is essentially independent of the thermal nonequilibrium. On the other hand, inspection of Figure 1 and Equation 3 indicates that Z could be extremely large during de-excitation due to the low translational temperature involved and $f^{AB}(i)$ giving higher weighting to k_d from the higher levels making the numerator in Equation 3 much larger than the denominator. Consequently, the dissociation rate may be accelerated to values comparable to the recombination rate making it important under some thermal nonequilibrium de-excitation conditions [19].

Hence, the current work looks to carry out a parametric study to identify nonequilibrium de-excitation conditions where the dissociation reaction is important and where it is not. Binary mixtures of O_2/O and N_2/N are studied in order to isolate the dissociation/recombination reactions. This follows recent studies on the recombination reaction in these mixtures using detailed kinetics simulations [14, 20, 21]. The current work

complements these works by using a continuum approach to look at the overall atomic recombination under nonequilibrium conditions.

II. Methodology

The current work is carried out via constant-volume heat bath simulations which are governed by

$$\begin{aligned} \frac{d\rho}{dt} &= 0 \\ \frac{dT_{tr}}{dt} &= 0 \\ \frac{dc_i}{dt} &= \frac{\dot{w}_i}{\rho} \end{aligned} \tag{4}$$

where t is the time, ρ is the mass density, c is the mass fraction, $\dot{w}$ is the mass production rate, and the subscript i is the species index. These are sets of ordinary differential equations (ODE) which are integrated using the Crank-Nicolson method given some starting condition. The gas is initially in equilibrium at some defined density, ρ_{ini}, and temperature, T_{ini}. The translational temperature is then instantaneously changed to some value, T_0, while the density either remains constant or is instantaneously changed to ρ_0 following a thermochemically frozen isentropic process from T_{ini} to T_0. From this starting condition, thermochemical relaxation governed by Equation 4 proceeds. Equilibration between the translational and rotational modes is assumed throughout. The test conditions are summarized in Table 1.

Table 1. The numerical test conditions. The letter following the condition number denotes the binary mixture (O for oxygen, N for nitrogen). $(c_{atom})_{ini}$ refers to the initial atomic mass fraction (equilibrium composition at ρ_{ini} and T_{ini})

Condition	T_{ini}, K	ρ_{ini}, kg/m^3	$(c_{atom})_{ini}$	T_0, K	ρ_0, kg/m^3
1O	4000	0.15	0.44	2000	0.15
1N	7000	0.15	0.23	2000	0.15
2O	2000	0.15	0.00	4000	0.15
2N	2000	0.15	0.00	7000	0.15
3O	4000	0.0015	0.97	2000	0.0015
3N	7000	0.0015	0.89	2000	0.0015
4O	4000	0.15	0.44	2000	0.0405
4N	7000	0.15	0.23	2000	0.0105
5O	7000	0.15	0.99	2000	0.15
5N	10000	0.15	0.90	2000	0.15
6O	4000	0.15	0.44	500	0.15
6N	7000	0.15	0.23	500	0.15
7O	4000	0.15	0.44	500	0.0030
7N	7000	0.15	0.23	500	0.00055
8O	7000	0.15	0.99	500	0.0028
8N	10000	0.15	0.90	500	0.0014
9O	4000	0.15	0.44	600	0.15
9N	7000	0.15	0.23	600	0.15
10O	4000	0.15	0.44	1000	0.15
10N	7000	0.15	0.23	1000	0.15

A State-to-State (StS) model, described in detail in Ref. [22-24], is used in the current work. The energies of the vibrational levels for N_2, and O_2 used in this work are obtained from the STELLAR database [25], and they are determined by solving the radial Schrödinger equation with potential curves obtained from the Rydberg-Klynning-Rees method [26]. There are 61 bound vibrational levels for N_2 and 46 for O_2. Only the ground electronic state is considered. The reactions modelled, consisting of vibration-vibration-translation (VVT), vibration-translation (VT), and vibration-dissociation (VD) reactions, are summarized in Table 2 and Table 3. The state-specific rates used originate from a combination of Forced Harmonic Oscillator (FHO) theory [27] and quasi-classical trajectory (QCT) calculations [28]. The accuracy of these rates is examined in Ref. [22-24]. The forward and backward rates are related by detailed balance using the partition functions. The average vibrational temperature can be obtained by solving the following equation for $T_{V,AB}$ [22, 24, 29],

$$\sum_i f^{AB}(i)E_{AB}(i) = \frac{\sum_i E_{AB}(i)\, exp\left(-\frac{E_{AB}(i)}{k_B T_{v,AB}}\right)}{\sum_i exp\left(-\frac{E_{AB}(i)}{k_B T_{v,AB}}\right)} \tag{5}$$

where the energy of the nonequilibrium vibrational distribution equals the energy of a Boltzmann equilibrium vibrational distribution at the vibrational temperature $T_{V,AB}$. Here, E is the level energy and k_B is the Boltzmann constant.

Table 2. The reactions considered in the oxygen binary mixture.

No.	Reaction	Model	Ref.
1	$O_2(i_1) + O_2(i_2) \leftrightarrow O_2(f_1) + O_2(f_2)$	FHO	[24]
2	$O_2(i) + O \leftrightarrow O_2(f) + O$	QCT	[28]
3	$O_2(i) + O_2 \leftrightarrow 2O + O_2$	FHO	[30]
4	$O_2(i) + O \leftrightarrow 3O$	QCT	[28]

Table 3. The reactions considered in the nitrogen binary mixture.

No.	Reaction	Model	Ref.
1	$N_2(i_1) + N_2(i_2) \leftrightarrow N_2(f_1) + N_2(f_2)$	FHO	[24]
2	$N_2(i) + N \leftrightarrow N_2(f) + N$	QCT	[13]
3	$N_2(i) + N_2 \leftrightarrow 2N + N_2$	FHO	[30]
4	$N_2(i) + N \leftrightarrow 3N$	QCT	[13]

Consider a molecular species $AB \in \{N_2, O_2\}$ at a vibrational level i_1, the resulting species mass production rate in a binary mixture can be written generally as [5, 31-33],

$$\dot{w_{AB(i_1)}} = \mathcal{M}_{AB}\left[\left\{\dot{w_{AB(i_1)}}\right\}_{VVT} + \left\{\dot{w_{AB(i_1)}}\right\}_{VT} + \left\{\dot{w_{AB(i_1)}}\right\}_{VD}\right] \tag{6}$$

where

$$\left\{\dot{w_{AB(i_1)}}\right\}_{VVT} = \sum_{i_2=0}^{i_{2,max}} \sum_{\substack{f_1=0 \\ f_1 \neq i_1}}^{f_{1,max}} \sum_{f_2=0}^{f_{2,max}} k_{VVT}(f_1, f_2 \rightarrow i_1, i_2) X_{f_1} X_{f_2} - k_{VVT}(i_1, i_2 \rightarrow f_1, f_2) X_{i_1} X_{i_2} \tag{7}$$

for the molecule-molecule interaction,

$$\left\{\dot{w_{AB(i_1)}}\right\}_{VT} = \sum_{M} \sum_{\substack{f_1=0 \\ f_1 \neq i_1}}^{f_{1,max}} k_{VT}(f_1, M \rightarrow i_1, M) X_{f_1} X_M - k_{VT}(i_1, M \rightarrow f_1, M) X_{i_1} X_M \tag{8}$$

for the molecule-atom interaction, and

$$\left\{\dot{w_{AB(i_1)}}\right\}_{VD} = \sum_{M} k_{VD}(A, B, M \rightarrow i_1, M) X_A X_B X_M - k_{VD}(i_1, M \rightarrow A, B, M) X_{i_1} X_M \tag{9}$$

for the vibration-dissociation reactions. Here A and B represent atomic species, $\mathcal{M}$ is the molar mass, k is the reaction rate coefficient (calculated from the FHO or QCT model depending on the reaction as stated in Table 2 and Table 3), and X is the molar concentration.

III. Results

The results for Condition 1 are shown in Figure 2 along with the corresponding thermal equilibrium (EQ) result in which $f^{AB}(i) = f_{eq}^{AB}(i, T_0)$ is defined making the VT and VVT reactions redundant and giving $Z = 1$ ($K_D = K_D^{EQ}$) throughout. The time when the normalized mass fraction (y-axis) reaches 0.5 differs between the nonequilibrium and equilibrium results by a factor of around 3.5 for oxygen and 2.0 for nitrogen; this is only a little smaller than that seen in the corresponding excitation conditions (around 5.0 for oxygen and 3.7 for nitrogen) shown in Figure 3 for Condition 2. Thus, Condition 1 can be considered to be substantially influenced by the dissociation reaction and, consequently, the thermal nonequilibrium. To provide further perspective, uncertainties of up to a factor of 6 [34] and an order of magnitude [10] is reported for first-principles calculated and experimentally measured dissociation rate constants, respectively, which would cause shifts in time of around the same amount (a factor of 6 and an order of magnitude) when put into the current context. Therefore, even when considering the bigger picture, the influence from thermal nonequilibrium should still be relevant despite being secondary compared to the uncertainty of the rates themselves in nonequilibrium simulations.

Let us define the ratio of the global dissociation rate $\dot{w_D}$ to the global recombination rate $\dot{w_R}$ as

$$\frac{\dot{w_D}}{\dot{w_R}} = \frac{\sum_i k_{VD}(i, M \rightarrow A, B, M) X_i X_M}{\sum_i k_{VD}(A, B, M \rightarrow i, M) X_A X_B X_M} \tag{10}$$

Examining Figure 2 (c) and (d), one can see that Condition 1 is influenced by the thermal nonequilibrium because Z attains a significant value in both of the dissociation reactions (both have a similar Z profile) which increases

the dissociation rate $\dot{w}_D$ to a value comparable (same order of magnitude) to the recombination rate $\dot{w}_R$. Such large values of Z are consistent with [7] who computed $Z \approx 10^{10}$ for similar conditions which indicates K_D has a much larger deviation from K_D^{EQ} here than those seen in excitation conditions where $Z \approx 10^{-2}$ as shown in Figure 3 and in [11, 16, 35].

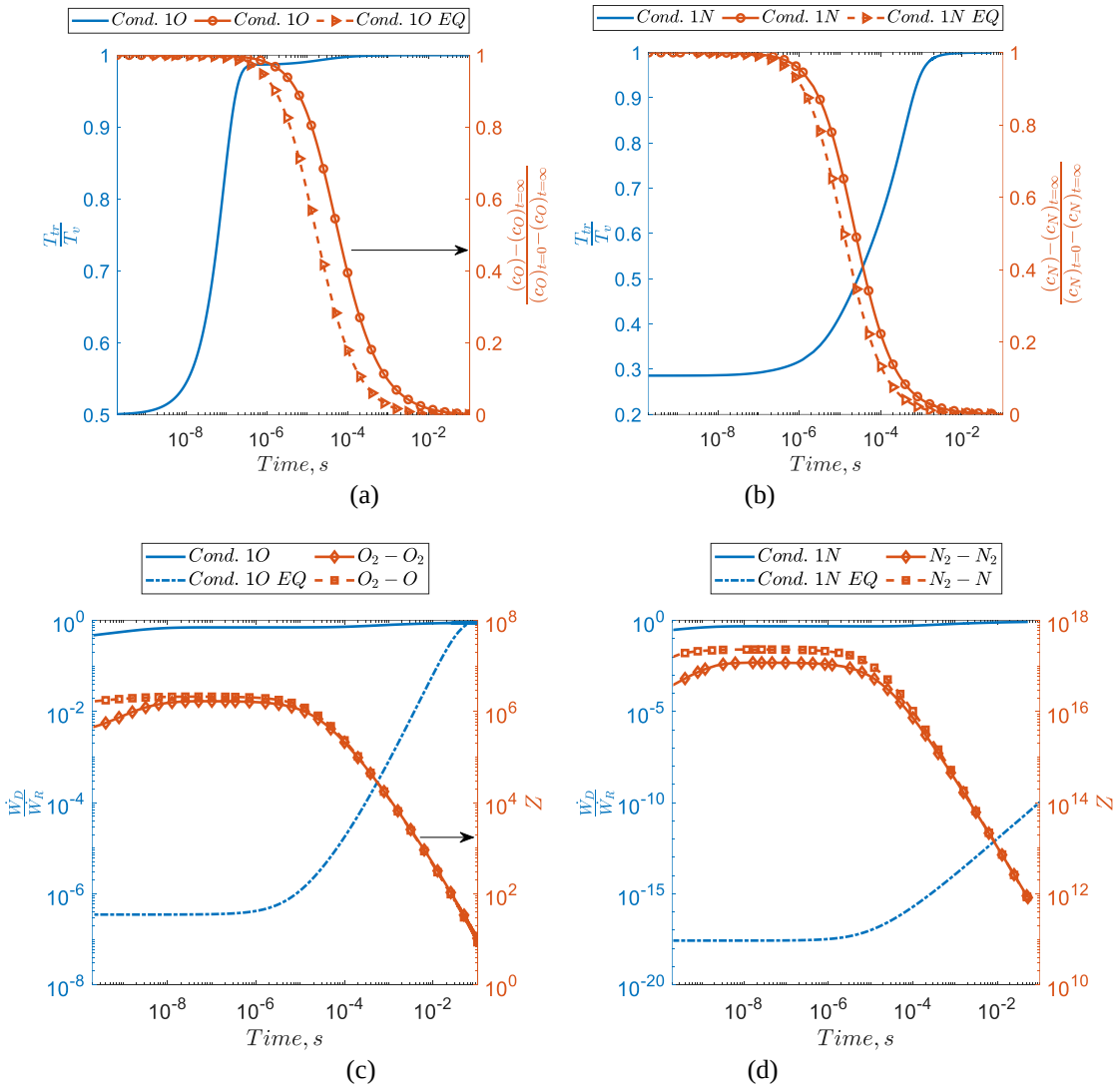

Figure 2. The normalized temperature ratio and atomic mass fraction for Conditions (a) 1O and (b) 1N, and the ratio between the dissociation and recombination rates ($\dot{w}_D/\dot{w}_R$) and Z for Conditions (c) 1O and (d) 1N. Z is calculated for reactions 3 and 4 in both Table 2 and Table 3. The colour of the lines matches the colour of the y-axis to which they belong.

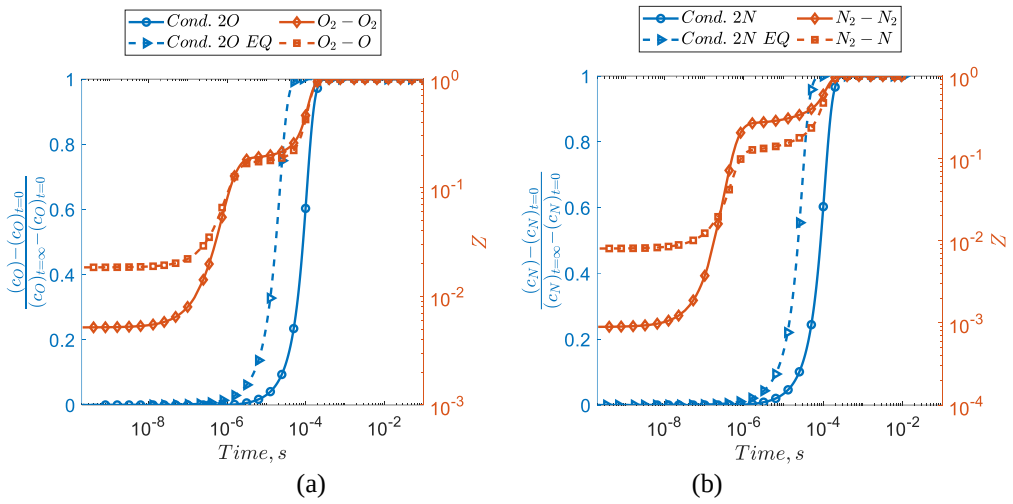

Figure 3. The normalized atomic mass fraction and *Z* for Conditions (a) 2O and (b) 2N.

In de-excitation conditions, as shown in Figure 2, Z maintains a large deviation from unity even when the average vibrational temperature T_v approximately equals the translational temperature ($t > 10^{-5}$ s for oxygen and $t > 10^{-3}$ s for nitrogen); this is due to the non-Boltzmann vibrational population distribution, as shown for example in Figure 4 for Condition 1O, which gets manifested spectacularly due to the extremely nonuniform distribution of k_d at the lower temperatures encountered during de-excitation as discussed in Section I. This result is consistent with [7] who earlier showed that Z is basically independent of T_v during de-excitation. In fact, Z is still of a significant value even when recombination essentially completes ($t \approx 10^{-2}$ s), as shown in Figure 2, because a non-Boltzmann distribution still exists at this point which requires further time to equilibrate, as shown for example in Figure 4 for Condition 1O. Such a prominent influence from non-Boltzmann distributions is not seen under excitation conditions as shown in Figure 3 and in [36, 37]. Subsequently, the existing simple analytical models for predicting Z under excitation conditions, which are designed to give $Z = 1$ when $T_{tr} = T_v$ [11, 15, 16], are inadequate for predicting Z under de-excitation conditions. Instead, more sophisticated models designed with consideration of de-excitation conditions, such as [10, 19], must be used in reduced-order modelling of de-excitation conditions such as Condition 1 where dissociation needs to be predicted accurately.

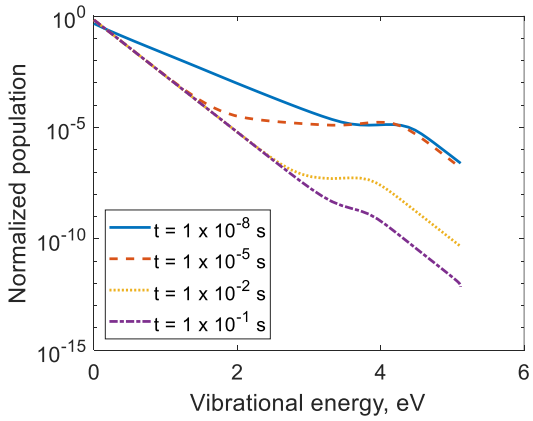

Figure 4. The normalized vibrational population distribution of O_2 in Condition 1O at different instances in time, t.

Beginning the parametric study, Figure 5 compares Condition 1 with its low-density equivalent: Condition 3. As demonstrated exemplarily for nitrogen, one can see in Figure 5 (a) that changing the density in this way does not appreciably change the degree of influence of thermal nonequilibrium on the overall atomic recombination; in both conditions, the nonequilibrium and equilibrium results differ in time by a factor of around 2.0. The same observation is made for oxygen. The reason for this is shown in Figure 5 (b): neither Z nor $\dot{w}_D/\dot{w}_R$ is changed in any significant way other than being shifted in time. Because the dissociation reaction is a second-order reaction while the recombination reaction is a third-order reaction, one may expect $\dot{w}_D/\dot{w}_R$ to increase when decreasing the density. However, this is not the case here because the initial equilibrium chemical composition is also adjusted accordingly with this lower density condition. That is, the initial chemical composition in Condition 3 is equilibrated with the lower density so the relaxation begins from a state with more dissociation which decreases $\dot{w}_D/\dot{w}_R$ thereby cancelling out the increase in $\dot{w}_D/\dot{w}_R$ from the lower density.

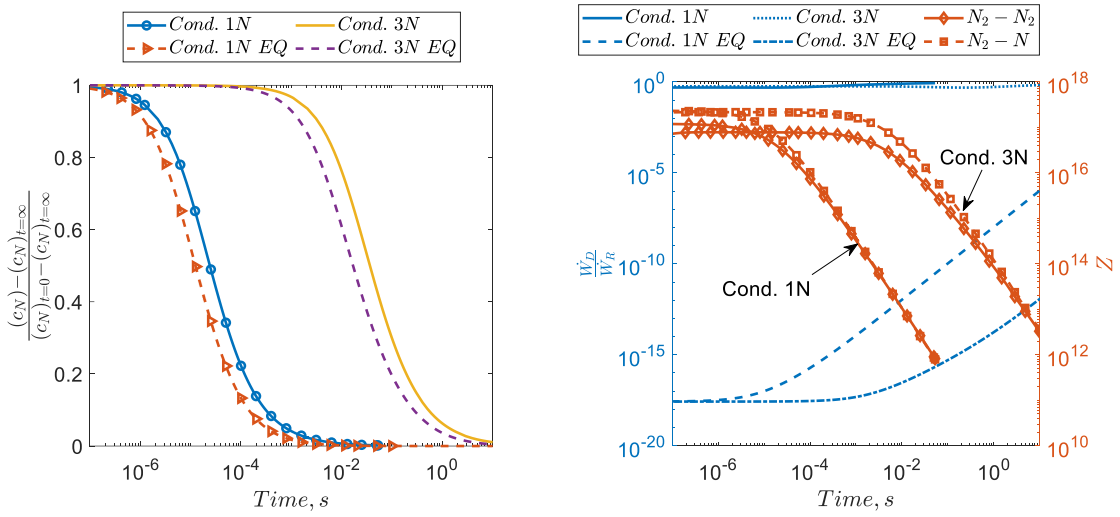

Figure 5. The (a) normalized atomic mass fraction and (b) ratio between the dissociation and recombination rates ($\dot{w}_D/\dot{w}_R$) and Z for the dissociation reaction with the molecular and atomic collision partners, for Conditions 1N and 3N.

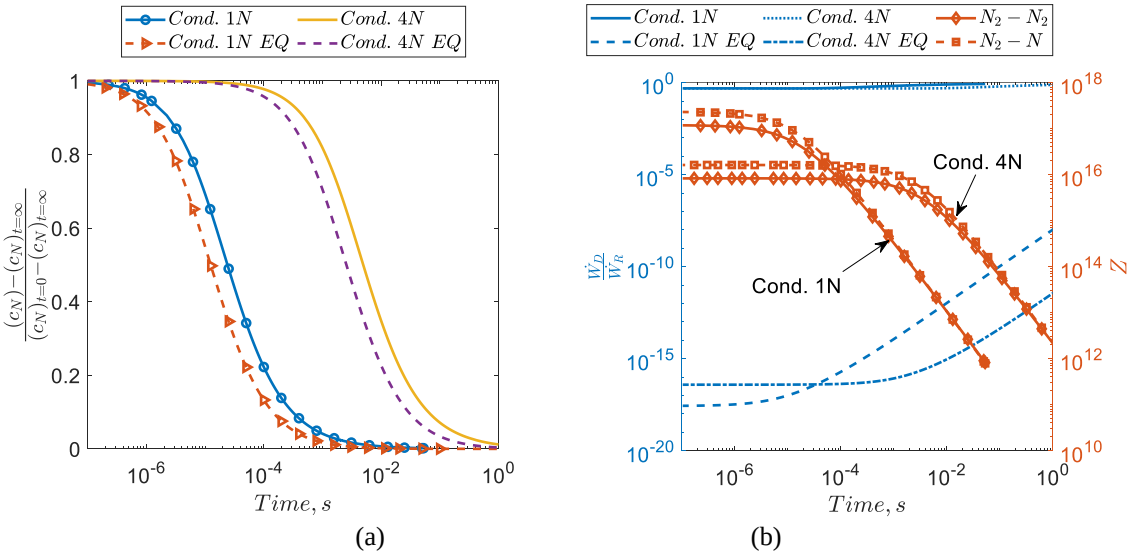

Figure 6. The (a) normalized atomic mass fraction and (b) ratio between the dissociation and recombination rates ($\dot{w}_D/\dot{w}_R$) and Z, for Conditions 1N and 4N.

Instead, to possibly observe the effect of changing density, one has to compare Condition 1 with Condition 4 where the density is reduced from ρ_{ini} to ρ_0 following a thermochemically frozen isentropic process consistent with the temperature change. This result is shown in Figure 6. Examining Figure 6 (b), the effect of lowering the density here in this way does indeed increase $\dot{w}_D/\dot{w}_R$ in the equilibrium result as expected. However, $\dot{w}_D/\dot{w}_R$ in the nonequilibrium result remain basically unchanged. This is because lowering the density is found to also lower Z, consistent with [7], which cancels out the increase in the equilibrium $\dot{w}_D/\dot{w}_R$ since the nonequilibrium $\dot{w}_D/\dot{w}_R$ is like the product of the equilibrium $\dot{w}_D/\dot{w}_R$ and Z. In [19], it was found that Z is heavily influenced by the

population of the upper vibrational energy levels, and the larger the upper level population the larger the Z. Hence, the lowering of Z from lowering the density is expected as lowering the density reduces the prominence of the (third-order) recombination reaction relative to the (second-order) dissociation reaction meaning that the upper levels get less populated (since molecules form at the upper levels) resulting in a less accelerated dissociation reaction. Consequently, changing the density in this way also does not appreciably change the degree of influence of thermal nonequilibrium on the overall atomic recombination as demonstrated for example in Figure 6 (a) for nitrogen, with the same observation made for oxygen.

A similar trend is observed when comparing Condition 1 with Condition 5 where the relaxation begins from a state with more thermochemical excitation. As demonstrated for example in Figure 7 for nitrogen, increasing the degree of excitation in the initial condition does not appreciably change the degree of influence of thermal nonequilibrium on the overall atomic recombination. This is because, although the larger degree of nonequilibrium increases Z as discussed in Section I and consistent with [7], it also decreases the equilibrium $\dot{w}_D/\dot{w}_R$ because the relaxation begins from a state with more dissociation resulting in the nonequilibrium $\dot{w}_D/\dot{w}_R$ being essentially unchanged. The same observation is found for oxygen.

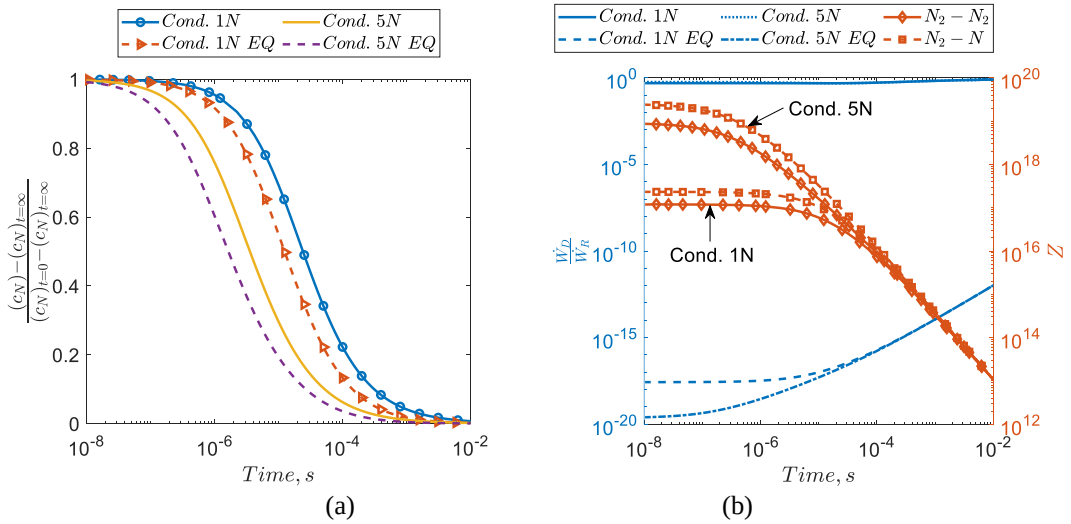

Figure 7. The (a) normalized atomic mass fraction and (b) ratio between the dissociation and recombination rates ($\dot{w}_D/\dot{w}_R$) and Z, for Conditions 1N and 5N.

Continuing with the parametric study, Figure 8 compares Condition 1 with its low-temperature equivalent: Condition 6. In this case, one can see that decreasing the isothermal translational temperature significantly decreases the degree of influence of thermal nonequilibrium on the overall atomic recombination as shown in Figure 8 (a) and (c) for Conditions 6O and 6N, respectively. For these two conditions, the equilibrium and nonequilibrium atomic mass fraction profiles are essentially the same for a significant portion of the relaxation,

and deviations only appear when approaching equilibrium when the dissociation reaction has to become important. Also shown in Figure 8 (a) and (c) are the corresponding results at intermediate isothermal translational temperatures of 600 K (Condition 9) and 1000 K (Condition 10). As expected, the results at these intermediate temperatures show intermediate degrees of influence from thermal nonequilibrium. This further confirms the aforementioned trend: increasing the isothermal translational temperature increases the influence of thermal nonequilibrium on the overall recombination.

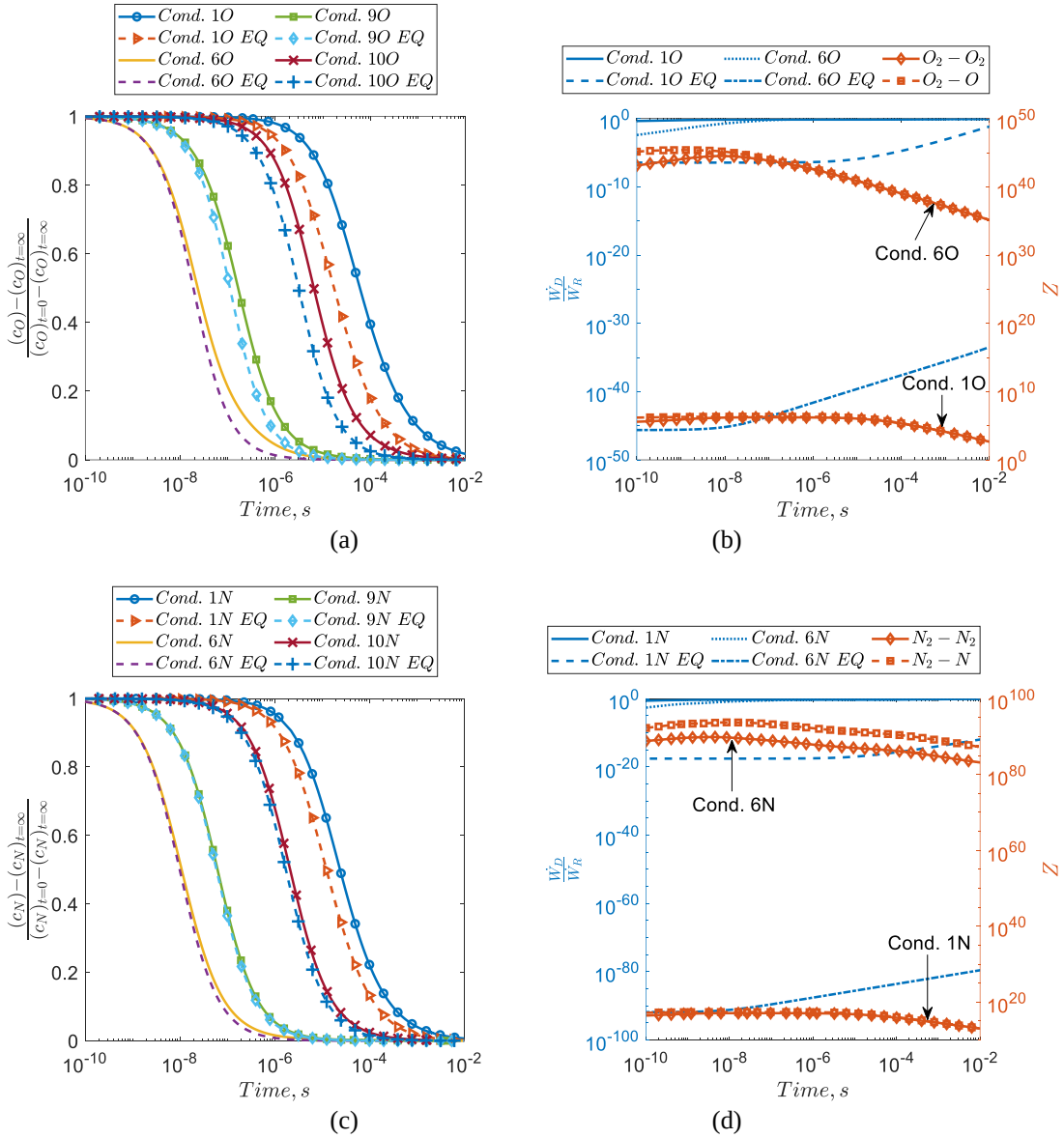

Figure 8. The normalized atomic mass fraction, ratio between the dissociation and recombination rates ($\dot{w}_D/\dot{w}_R$), and Z for the specified conditions.

Examining Figure 8 (b) and (d), significantly larger Z is produced in the lower temperature conditions as expected due to the extremely nonuniform distribution of k_d at lower temperatures as mentioned in section I. However, at the lower temperatures, the equilibrium constant becomes very small, as shown in Figure 9, causing

the equilibrium $\dot{w}_D/\dot{w}_R$ to be very small which more than offsets the increase in Z resulting in the recombination rate being more than an order of magnitude greater than the nonequilibrium dissociation rate during the majority of the atomic recombination in the nonequilibrium results. Here, unlike in the scenarios presented earlier, the two competing processes do not completely cancel each other out as the decrease in the equilibrium $\dot{w}_D/\dot{w}_R$ wins over the increase in Z. Consequently, the dissociation has little influence on the overall reaction and, thus, does not need to be predicted accurately in this case in reduced-order modelling.

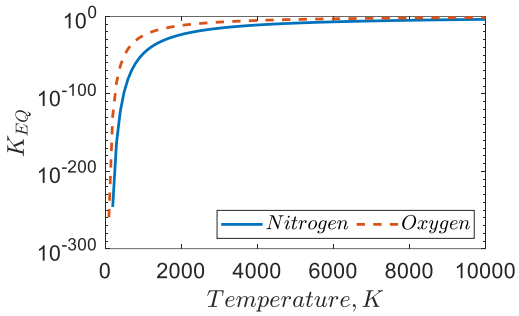

Figure 9. The equilibrium constant for the oxygen and nitrogen dissociation/recombination reactions calculated using the partition functions.

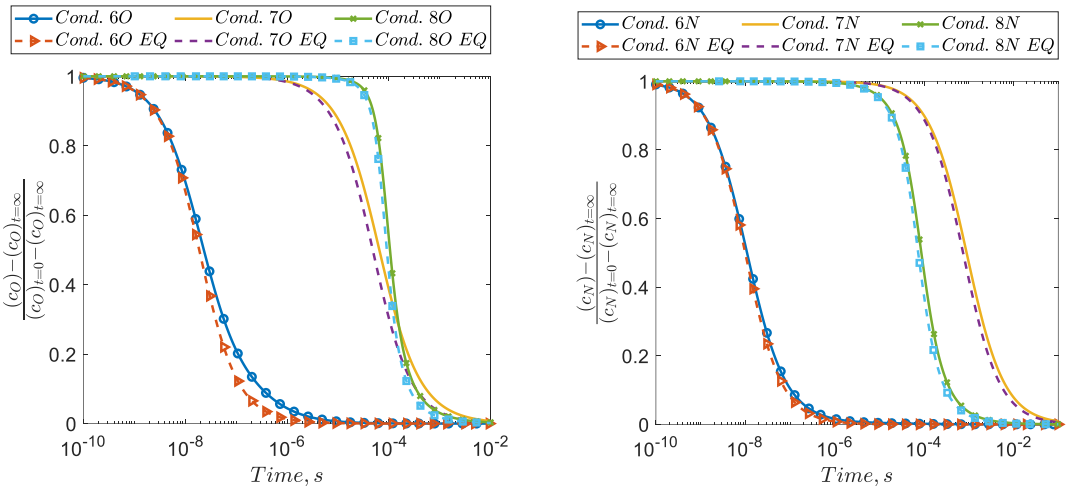

Figure 10. The normalized atomic mass fraction for the specified (a) oxygen and (b) nitrogen conditions.

The current parametric study indicates that the translational temperature at which the de-excitation occurs is the most important parameter influencing the sensitivity of the overall atomic recombination to the thermal nonequilibrium. To further confirm this result, additional simulations are performed at two variations of the low-temperature condition: Conditions 7 and 8. In Condition 7, ρ_0 is obtained from ρ_{ini} following a frozen isentropic process from T_{ini} to T_0. Condition 8 is similar to condition 7 except it has a higher value of T_{ini} meaning the relaxation begins from a state with more thermochemical excitation. The results are shown in Figure 10, and one can see that the overall atomic recombination has little sensitivity to the thermal nonequilibrium in all these low-

temperature cases due to the very small value of K_{EQ}, which causes K_R to be very large according to Equation 1, making the dissociation reaction less important. Further demonstrating the importance of K_{EQ}, the results throughout this work show that the nitrogen recombination is always less sensitive to the thermal nonequilibrium than the oxygen recombination under comparable conditions because nitrogen always has a lower value of K_{EQ} than oxygen at any given temperature as shown in Figure 9.

IV. Implications

In light of the current findings, it can be suggested that in O_2/O and N_2/N de-excitation at higher translational temperatures, it is important to accurately predict the dissociation reaction to determine the overall atomic recombination process correctly when performing reduced-order modelling; this can potentially be done using models such as [10, 19]. Detailed treatment of the dissociation reaction may be unnecessary at lower translational temperatures for accurately determining the overall atomic recombination. Regarding air de-excitation, the current results for binary mixtures would be irrelevant because, during de-excitation, the NO exchange reactions are known to (1) play an influential role in determining the amount of oxygen and nitrogen [4, 18, 38, 39], and (2) be heavily influenced by thermal nonequilibrium [40, 41]. Consider the reaction $N_2 + O \leftrightarrow NO + N$ with the vibrational state-specific reaction $N_2(i) + O \leftrightarrow NO(j) + N$ where i and j are the vibrational levels of N_2 and NO, respectively, one can write, following [10],

$$K_F = \sum_j \sum_i k_f(i,j) f^{N2}(i)$$
$$K_B = \sum_j \sum_i k_b(i,j) f^{NO}(j) = \sum_j \sum_i \frac{k_f(i,j)}{K_{EQ}(T_{tr})} \frac{f^{NO}(j) f_{eq}^{N2}(i,T_{tr})}{f_{eq}^{NO}(j,T_{tr})} \quad (11)$$

where subscript ‘f’ or ‘F’ refers to the reaction direction of *NO* production, and vice versa for subscript ‘b’ or ‘B’. As shown in Figure 11, k_f has obvious nonuniformity, which increases with decreasing temperature, like with the dissociation reaction. Hence, Equation 11 indicates that both directions of the *NO* exchange reaction would be influenced by the nonequilibrium vibrational population distribution *f*. The same is the case for the other *NO* exchange reaction. Therefore, thermal nonequilibrium would always influence the oxygen and nitrogen kinetics under any air de-excitation condition.

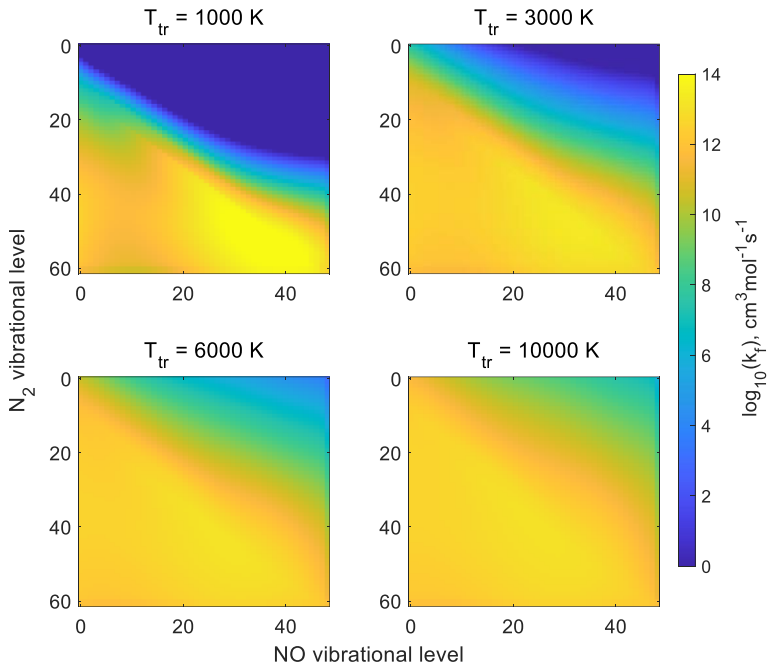

Figure 11. The state-specific rate constants for $N_2(i) + O \rightarrow NO(f) + N$ obtained via QCT in [42].

Nonetheless, the fact that it is possible to find conditions for a binary mixture where the overall chemical relaxation is independent of the thermal relaxation is an important result. This result can be taken advantage of for the experimental determination of the equilibrium dissociation/recombination rates. Doubts have been raised decades ago by Rice [43], and continue to be expressed recently by Singh & Schwartzentruber [10], as to whether the existing experimental dissociation rates, basically all measured using the shock tube method, actually correspond to the thermal equilibrium dissociation rates. Therefore, in light of the current results, Wilson's technique [44, 45], shown in Figure 12 (a), is strongly recommended as an alternative experimental method to the shock tube method for determining the equilibrium dissociation/recombination rates. In Wilson's technique, the double Prandtl-Meyer expansion can be designed to manufacture an essentially frozen isentropic flow which rapidly decreases the translational temperature of some thermochemically excited flow to some low value, and thermochemical relaxation occurs subsequently in the one-dimensional channel. By diluting the binary mixture with an inert gas such as argon or helium, a low translational temperature can be maintained during the relaxation which is necessary to prevent the overall atomic recombination process from being influenced by the thermal nonequilibrium. The one-dimensional centered rarefaction technique [46, 47] can be used as an alternative to Wilson's technique. In this technique, shown in Figure 12 (b), the portion of the initially excited flow that passes near the center of the rarefaction can be designed to undergo an essentially frozen isentropic expansion before thermochemical relaxation occurs in a one-dimensional channel. In both techniques, measurement of the overall

atomic recombination would allow the equilibrium recombination rate to be confidently determined which can then be related to the equilibrium dissociation rate via K_{EQ}. Subsequent comparisons with rates obtained from shock tube experiments and first-principles calculations would be extremely interesting. Additionally, the experimental results obtained at low temperatures will complement the shock tube results, which are obtained at high temperatures, giving the existing experimental database completeness.

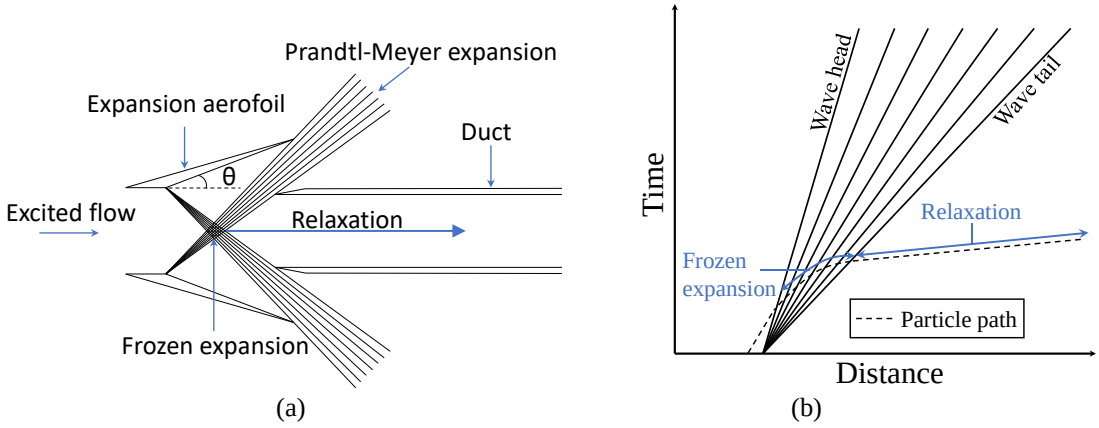

Figure 12. The (a) Wilson's, and (b) one-dimensional centered rarefaction methods.

Such a dilution mentioned above is not expected to significantly influence the sensitivity of the recombination to thermal nonequilibrium at a given temperature because this depends on Z and Z is not sensitive to the collision partner, as shown throughout the current work with Z being similar among the atomic and molecular collision partners, since the normalized distribution of $k_d(i)$ at a given temperature is not sensitive to the collision partner [48]. Z could be influenced by the vibrational relaxation, which is dependent on the collision partner, but this influence is not expected to be significant. To further examine the influence of dilution, simulations of the conditions shown in Table 4 are performed. Because StS rates for the inert gas collisions are currently unavailable, 0.95 mole fraction of N_2 or N and O_2 or O are used as a diluent in O_2/O and N_2/N, respectively, where it is treated as a monoatomic inert species which take part only as a collision partner in the dissociation/recombination reaction. When N_2 or O_2 is used as the diluent, it is treated as a monoatomic inert species in the thermal reactions too so that, instead of being involved via VVT reactions, it is involved via VT reactions. The $O_2(i_1) + O_2 \leftrightarrow O_2(f_1) + O_2$ and $N_2(i_1) + N_2 \leftrightarrow N_2(f_1) + N_2$ VT rates necessary to perform simulation of Conditions 10O and 10N, respectively, are obtained from the STELLAR database [25], which are calculated using FHO theory. The results are shown in Figure 13; one can see that the overall recombination process in O_2/O and N_2/N is essentially uninfluenced by the thermal nonequilibrium as long as the temperature is low, regardless of which species is used as the diluent.

Table 4. The numerical test conditions with dilution. The diluent has a 0.95 mole fraction in all cases. ρ_{ini} to ρ_0 follows a thermochemically frozen isentropic process from T_{ini} to T_0.

Condition	T_{ini}, K	ρ_{ini}, kg/m^3	T_0, K	ρ_0, kg/m^3	Diluent
9O	7000	15	500	0.29	O
9N	10000	15	500	0.16	N
10O	7000	15	500	0.023	O_2
10N	10000	15	500	0.0096	N_2

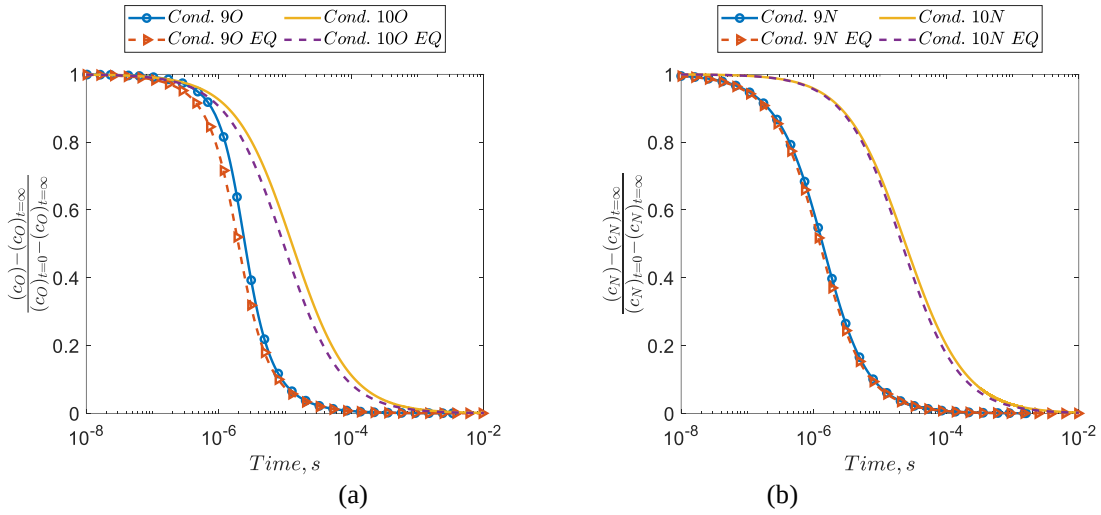

Figure 13. The normalized atomic mass fraction for the specified (a) oxygen and (b) nitrogen conditions.

V. Conclusions

A parametric study is carried out via StS constant-volume heat bath simulations for binary mixtures of O_2/O and N_2/N to identify nonequilibrium de-excitation conditions where the overall atomic recombination is influenced by thermal nonequilibrium and where it is not. Parameters examined include the density, degree of initial excitation, and translational temperature. It is found that the translational temperature is the most important parameter influencing the sensitivity of the overall atomic recombination to the thermal nonequilibrium. At a higher translational temperature of 2000 K, the overall atomic recombination process is influenced by the thermal nonequilibrium to an extent that is comparable to that seen in the corresponding excitation conditions. In this case, it is important to accurately predict the nonequilibrium dissociation reaction when performing reduced-order modelling. A low translational temperature of around 500 K is found to prevent the overall atomic recombination process from being influenced by the thermal nonequilibrium due to the small value of K_{EQ} making the dissociation reaction less important. Consequently, in this case, detailed treatment of the dissociation reaction in reduced-order modelling may be unnecessary for accurately determining the overall atomic recombination. This important result can be further taken advantage of for the experimental determination of the equilibrium dissociation/recombination rates which would be extremely useful. Dilution is not found to influence this result

to any significant extent. Work is already underway by the current authors to generate StS rates for the inert gas collisions which will then be used to design these experiments to be eventually conducted in a high-enthalpy impulse facility. For air de-excitation, thermal nonequilibrium will always play an important role in the oxygen and nitrogen kinetics due to the existence of the *NO* exchange reactions.

Acknowledgements

This work was supported by the Hong Kong Research Grants Council (No. 15206522).

Data Availability Statement

The data that supports the findings of this study are available within the article. For convenience, in case the reader wishes to independently verify the presented results, the raw data for Condition 1N can be downloaded here which can be used to derive the properties presented in this paper to exemplarily check the work.

References

[1] J. W. Rich, S. O. Macheret, and I. V. Adamovich, "Aerothermodynamics of vibrationally nonequilibrium gases," *Experimental Thermal and Fluid Science,* vol. 13, no. 1, pp. 1-10, 1996, doi: https://doi.org/10.1016/0894-1777(95)00128-X.

[2] C. Park and S.-H. Lee, "Validation of multitemperature nozzle flow code," *Journal of Thermophysics and Heat Transfer,* vol. 9, no. 1, pp. 9-16, 1995, doi: https://doi.org/10.2514/3.622.

[3] M. J. Wright, F. S. Milos, and P. Tran, "Afterbody aeroheating flight data for planetary probe thermal protection system design," *Journal of Spacecraft and Rockets,* vol. 43, no. 5, pp. 929-943, 2006, doi: https://doi.org/10.2514/1.17703.

[4] C. Park, *Nonequilibrium Hypersonic Aerothermodynamics*. New York: Wiley, 1989, p. 358.

[5] C. Park, "Thermochemical relaxation in shock tunnels," *Journal of Thermophysics and Heat Transfer,* vol. 20, no. 4, pp. 689-698, 2006, doi: https://doi.org/10.2514/1.22719.

[6] S. Gu, J. Hao, Q. Wang, and C.-Y. Wen, "Influence of thermochemical nonequilibrium on expansion tube air test conditions: A numerical study," *Physics of Fluids,* vol. 35, no. 3, 2023, doi: https://doi.org/10.1063/5.0141281.

[7] G. Colonna, I. Armenise, D. Bruno, and M. Capitelli, "Reduction of state-to-state kinetics to macroscopic models in hypersonic flows," *Journal of Thermophysics and Heat Transfer,* vol. 20, no. 3, pp. 477-486, 2006, doi: https://doi.org/10.2514/1.18377.

[8] C. Park, "Review of chemical-kinetic problems of future NASA missions. I-Earth entries," *Journal of Thermophysics and Heat Transfer,* vol. 7, no. 3, pp. 385-398, 1993, doi: https://doi.org/10.2514/3.431.

[9] J. G. Hall and C. E. Treanor, "Nonequilibrium effects in supersonic-nozzle flows," AGARDograph No. 124, 1967. [Online]. Available: https://www.sto.nato.int/publications/AGARD/AGARD-AG-124/AGARD-AG-124.pdf

[10] N. Singh and T. E. Schwartzentruber, "Nonequilibrium dissociation and recombination models for hypersonic flows," *AIAA Journal,* vol. 60, no. 5, pp. 1-16, 2022, doi: https://doi.org/10.2514/1.J061154.

[11] J. Hao, J. Wang, and C. Lee, "Assessment of vibration–dissociation coupling models for hypersonic nonequilibrium simulations," *Aerospace Science and Technology*, vol. 67, pp. 433-442, 2017, doi: https://doi.org/10.1016/j.ast.2017.04.027.

[12] S. P. Sharma, W. M. Huo, and C. Park, "Rate parameters for coupled vibration-dissociation in a generalized SSH approximation," *Journal of Thermophysics and Heat Transfer*, vol. 6, no. 1, pp. 9-21, 1992, doi: https://doi.org/10.2514/3.312.

[13] F. Esposito, I. Armenise, and M. Capitelli, "N–N2 state to state vibrational-relaxation and dissociation rates based on quasiclassical calculations," *Chemical Physics*, vol. 331, no. 1, pp. 1-8, 2006, doi: https://doi.org/10.1016/j.chemphys.2006.09.035.

[14] E. C. Geistfeld, E. Torres, and T. Schwartzentruber, "Quasi-classical trajectory analysis of three-body collision induced recombination in neutral nitrogen and oxygen," *The Journal of Chemical Physics*, vol. 159, no. 15, 2023, doi: https://doi.org/10.1063/5.0163942.

[15] R. S. Chaudhry and I. D. Boyd, "Parametric comparison of the Park and MMT chemical kinetics models with multiple freestream speeds," presented at the AIAA Aviation 2023 Forum, San Diego, CA, 12-16 June, 2023, AIAA Paper 2023-3621, doi: https://doi.org/10.2514/6.2023-3621.

[16] I. Arsentiev, B. Loukhovitski, and A. Starik, "Application of state-to-state approach in estimation of thermally nonequilibrium reaction rate constants in mode approximation," *Chemical Physics*, vol. 398, pp. 73-80, April 2012, doi: https://doi.org/10.1016/j.chemphys.2011.06.011.

[17] E. Kustova, E. Nagnibeda, T. Y. Alexandrova, and A. Chikhaoui, "Non-equilibrium dissociation rates in expanding flows," *Chemical Physics Letters*, vol. 377, no. 5-6, pp. 663-671, 2003, doi: https://doi.org/10.1016/S0009-2614(03)01213-2.

[18] A. Chikhaoui, E. Nagnibeda, E. Kustova, and T. Y. Alexandrova, "Modeling of dissociation–recombination in nozzles using strongly non-equilibrium vibrational distributions," *Chemical Physics*, vol. 263, no. 1, pp. 111-126, 2001, doi: https://doi.org/10.1016/S0301-0104(00)00345-1.

[19] G. Colonna, L. D. Pietanza, and M. Capitelli, "Recombination-assisted nitrogen dissociation rates under nonequilibrium conditions," *Journal of Thermophysics and Heat Transfer*, vol. 22, no. 3, pp. 399-406, 2008, doi: https://doi.org/10.2514/1.33505.

[20] C. Kondur and K. A. Stephani, "Rate constants and molecular recombination pathways of oxygen from quasi-classical trajectory simulations of the O3 system," *Chemical Physics*, vol. 552, p. 111357, January 2022, doi: https://doi.org/10.1016/j.chemphys.2021.111357.

[21] C. Kondur and K. A. Stephani, "Effects of the third body (O and N) on the recombination of molecular nitrogen using quasi-classical trajectory methods," *Chemical Physics*, vol. 576, p. 112092, January 2024, doi: https://doi.org/10.1016/j.chemphys.2023.112092.

[22] S. Gu, J. Hao, and C.-Y. Wen, "State-specific study of air in the expansion tunnel nozzle and test section," *AIAA Journal*, vol. 60, no. 7, pp. 4024-4038, 2022, doi: https://doi.org/10.2514/1.J061479.

[23] S. Gu, J. Hao, and C.-Y. Wen, "Can vibrational pumping occur via O2–N2 collisions in nonequilibrium vibrationally excited air?," *Physics of Fluids*, vol. 35, no. 6, 2023, doi: https://doi.org/10.1063/5.0151461.

[24] S. Gu, J. Hao, and C.-Y. Wen, "On the vibrational state-specific modelling of radiating normal-shocks in air," *AIAA Journal*, vol. 60, no. 6, pp. 3760-3774, 2022, doi: https://doi.org/10.2514/1.J061438.

[25] M. Lino da Silva, J. Loureiro, and V. Guerra, "A multiquantum dataset for vibrational excitation and dissociation in high-temperature O2–O2 collisions," *Chemical Physics Letters*, vol. 531, pp. 28-33, 2012, doi: https://doi.org/10.1016/j.cplett.2012.01.074.

[26] M. Lino da Silva, V. Guerra, and J. Loureiro, "State-resolved dissociation rates for extremely nonequilibrium atmospheric entries," *Journal of Thermophysics and Heat Transfer*, vol. 21, no. 1, pp. 40-49, 2007, doi: https://doi.org/10.2514/1.24114.

[27] I. V. Adamovich, S. O. Macheret, J. W. Rich, and C. E. Treanor, "Vibrational energy transfer rates using a forced harmonic oscillator model," *Journal of Thermophysics and Heat Transfer*, vol. 12, no. 1, pp. 57-65, 1998, doi: https://doi.org/10.2514/2.6302.

[28] F. Esposito and M. Capitelli, "The relaxation of vibrationally excited O2 molecules by atomic oxygen," *Chemical Physics Letters*, vol. 443, no. 4-6, pp. 222-226, 2007, doi: https://doi.org/10.1016/j.cplett.2007.06.099.

[29] A. Guy, A. Bourdon, and M.-Y. Perrin, "Consistent multi-internal-temperatures models for nonequilibrium nozzle flows," *Chemical Physics*, vol. 420, pp. 15-24, 2013, doi: https://doi.org/10.1016/j.chemphys.2013.04.018.

[30] M. Lino da Silva, B. Lopez, V. Guerra, and J. Loureiro, "A multiquantum state-to-state model for the fundamental states of air: the stellar database," in *Proceedings of 5th International Workshop on Radiation of High Temperature Gases in Atmospheric Entry*, Barcelona, Spain, 16-19 October 2012, vol. 714, Noordwijk, The Netherlands: ESASP, p. 16.

[31] J. Hao, J. Wang, and C. Lee, "State-specific simulation of oxygen vibrational excitation and dissociation behind a normal shock," *Chemical Physics Letters*, vol. 681, pp. 69-74, August 2017, doi: https://doi.org/10.1016/j.cplett.2017.05.042.

[32] M. S. Grover, P. Valentini, E. Josyula, and R. S. Chaudhry, "Vibrational state-to-state and multiquantum effects for N2+ N2 interactions at high temperatures for aerothermodynamic applications," presented at the AIAA Scitech 2020 Forum, Orlando, FL, 6-10 January, 2020, AIAA Paper 2020-1227, doi: https://doi.org/10.2514/6.2020-1227.

[33] B. Lopez and M. Lino Da Silva, "Non-Boltzmann analysis of hypersonic air re-entry flows," presented at the 11th AIAA/ASME Joint Thermophysics and Heat Transfer Conference, Atlanta, GA, 16-20 June, 2014, AIAA Paper 2014-2547, doi: https://doi.org/10.2514/6.2014-2547.

[34] S. Venturi, R. Jaffe, and M. Panesi, "Bayesian machine learning approach to the quantification of uncertainties on ab initio potential energy surfaces," *The Journal of Physical Chemistry A*, vol. 124, no. 25, pp. 5129-5146, 2020, doi: https://doi.org/10.1021/acs.jpca.0c02395.

[35] R. S. Chaudhry and G. V. Candler, "Statistical analyses of quasiclassical trajectory data for air dissociation," presented at the AIAA Scitech 2019 Forum, San Diego, California, 2019, AIAA Paper 2019-0789, doi: https://doi.org/10.2514/6.2019-0789.

[36] J. Hao and C.-Y. Wen, "Maximum entropy modeling of oxygen vibrational excitation and dissociation," *Physical Review Fluids*, vol. 4, no. 5, p. 053401, 2019, doi: https://doi.org/10.1103/PhysRevFluids.4.053401.

[37] R. S. Chaudhry, I. D. Boyd, E. Torres, T. E. Schwartzentruber, and G. V. Candler, "Implementation of a chemical kinetics model for hypersonic flows in air for high-performance CFD," presented at the AIAA Scitech 2020 Forum, Orlando, FL, 2020, AIAA Paper 2020-2191, doi: https://doi.org/10.2514/6.2020-2191.

[38] G. Colonna, M. Tuttafesta, M. Capitelli, and D. Giordano, "Non-Arrhenius NO formation rate in one-dimensional nozzle airflow," *Journal of Thermophysics and Heat Transfer*, vol. 13, no. 3, pp. 372-375, 1999, doi: https://doi.org/10.2514/2.6448.

[39] A. Q. Eschenroeder, D. W. Boyer, and J. G. Hall, "Nonequilibrium expansions of air with coupled chemical reactions," *Physics of Fluids*, vol. 5, no. 5, pp. 615-624, 1962, doi: https://doi.org/10.1063/1.1706665.

[40] S. Séror, E. Schall, M.-C. Druguet, and D. Zeitoun, "An extension of CVDV model to Zeldovich exchange reactions for hypersonic non-equilibrium air flows," *Shock waves*, vol. 8, no. 5, pp. 285-298, 1998, doi: https://doi.org/10.1007/s001930050121.

[41] O. Knab, H.-H. Fruehauf, and E. Messerschmid, "Theory and validation of the physically consistent coupled vibration-chemistry-vibration model," *Journal of Thermophysics and Heat Transfer*, vol. 9, no. 2, pp. 219-226, 1995, doi: https://doi.org/10.2514/3.649.

[42] F. Esposito and I. Armenise, "Reactive, inelastic, and dissociation processes in collisions of atomic oxygen with molecular nitrogen," *The Journal of Physical Chemistry A*, vol. 121, no. 33, pp. 6211-6219, 2017, doi: https://doi.org/10.1021/acs.jpca.7b04442.

[43] O. Rice, "On the relation between an equilibrium constant and the nonequilibrium rate constants of direct and reverse reactions," *The Journal of Physical Chemistry*, vol. 65, no. 11, pp. 1972-1976, 1961, doi: https://doi.org/10.1021/j100828a014.

[44] J. Wilson, "An experiment to measure the recombination rate of oxygen," *Journal of Fluid Mechanics*, vol. 15, no. 4, pp. 497-512, 1963, doi: https://doi.org/10.1017/S0022112063000410.

[45] M. Slack, K. Bray, R. East, and N. Pratt, "Steady expansion of shock‐heated gases for recombination studies," *Physics of Fluids*, vol. 12, no. 5, pp. I-113-I-117, 1969, doi: https://doi.org/10.1063/1.1692588.

[46] A. E. Nasser and J. W. Cleaver, "Vibrational relaxation of carbon monoxide in an unsteady expansion wave," *Acta Astronautica*, vol. 4, no. 3-4, pp. 357-373, 1977, doi: https://doi.org/10.1016/0094-5765(77)90056-X.

[47] W. Beck and J. Mackie, "Application of the shock tube unsteady expansion wave technique to the study of chemical reactions," *Journal of Physics D: Applied Physics*, vol. 11, no. 9, p. 1249, 1978, doi: 10.1088/0022-3727/11/9/003.

[48] P. Mariotto *et al.*, "Vibrational state-to-state modeling of a recombining nitrogen/argon plasma," presented at the AIAA Scitech 2019 Forum, San Diego, California, 7-11 January, 2019, AIAA 2019-0796, doi: https://doi.org/10.2514/6.2019-0796.